Scanning Microscopy

Volume 2 | Number 4 Article 11

10-4-1988

Backscattered Electrons and Their Influence on Contrast in the Scanning Electron Microscope

F. Hasselbach
Universität Tübingen

H. -R. Krauss
Universität Tübingen

Scanning Microscopy, Vol. 2, No. 4, 1988 (Pages 1947-1956)
Scanning Microscopy International, Chicago (AMF O'Hare), IL 60666 USA

0891-7035/88$3.00+.00

BACKSCATTERED ELECTRONS AND THEIR INFLUENCE ON CONTRAST IN THE SCANNING ELECTRON MICROSCOPE

F. Hasselbach* and H.-R. Krauss

Institut für Angewandte Physik der Universität Tübingen
Auf der Morgenstelle 12, D-7400 Tübingen, West Germany

(Received for publication February 27, 1988, and in revised form October 04, 1988)

Abstract

The backscattered electron (BSE) induced secondaries (SE2) emerge from an area that is usually many orders of magnitude larger than the area in which the impinging primary probe releases secondary electrons (SE1). These SE2 secondary electrons form a) an undesired background signal in high resolution scanning micrographs and b) are responsible for the well known proximity effect in electron beam lithography. In this paper we focus our attention on the first topic exclusively: we discuss the complex influence of the SE2 on contrast in SEM micrographs (neglecting the components SE3 and SE4). We do this on the basis of our emission-microscopic measurements of the spatial distributions of SE1 and SE2 emerging from flat bulk specimens. By integrating these distributions in two dimensions we calculate the total number of SE1 and SE2 electrons and deduce the signal to backgroud ratio SE1/(SE1+SE2), i.e., the maximum contrast in one pixel ("single pixel contrast") and the contrast of two adjacent pixels 1 and 2 according to its usual definition $C=(I_1-I_2)/(I_1+I_2)$. We calculate the enhanced secondary emission factor β for backscattered electrons from our total numbers of SE1 and SE2 for Si, Ge and Ag to $\beta_{Si}=2.58$, $\beta_{Ge}=1.46$, $\beta_{Ag}=1,23$.

Key words: Scanning electron microscopy, contrast formation, influence of SE2 on contrast, spatial distribution of the SE1 and SE2, electron beam lithography, proximity effect, backscattering of electrons, β values, emission microscopy.

*Address for correspondence:
Franz Hasselbach
Institut für Angewandte Physik
Auf der Morgenstelle 12
D-7400 Tübingen
West Germany
Phone No.: Germany/7071/296328

Introduction

Contrast formation in scanning electron microscopy (SEM) of bulk specimens is very complex, in particular in the "secondary-electron-mode" where the secondaries are used to make up the video signal. The reason for this complexity is that - unlike in transmission electron microscopy or light microscopy - the source of the image forming electrons, here secondary electrons, is not exclusively located in the pixel just scanned by the electron beam (e.g., Everhart et al. 1959; Seiler 1968, 1983; Reimer et al. 1968; Robinson 1974; George and Robinson 1976). Instead, the total of the secondaries has a spatially very extended origin. According to their origin they are usually divided into the following categories: 1) the part SE1 containing highly resolved information about the specimen surface since these secondaries are released by the incident primary beam inside the area of the pixel just scanned (without regard to present-day extremely high resolution scanning microscopes which reach spot sizes smaller than the exit depth and the range of the secondary electrons in the specimen) and 2) the fractions SE2 and SE3. These parts contain no highly resolved information: the portion SE2, released by the backscattered electrons (BSE's) when leaving the specimen surface, emerge from a rather extended region around the impinging beam (e.g., Pease 1965; Hasselbach 1971, 1973; Yamamoto 1976). Thereafter they hit the walls of the specimen chamber and the pole piece of the last lens generating an extremely extended source of secondaries well known as fraction SE3. The SE2 and SE3 make up a considerable part of the amplitude of the video signal if they are not prevented from reaching the detector by special detectors (e.g., Hasselbach et al.1983) or specimen geometry. Their amplitude is superposed to the highly resolved SE1 signal and

acts as a slowly varying noise signal.

The aim of this paper is to calculate quantitatively the influence of the SE2 electrons on contrast in scanning electron micrographs. We do this on the basis of data of the spatial distributions of SE1 and SE2 which we have measured using our emission microscopical method (Hasselbach 1971, 1973; Hasselbach and Rieke 1978, 1982; Hasselbach and Krauß 1985). These measurements were made on model specimens consisting of bulk silicon, germanium and silver either highly polished or evaporated on polished glass substrates. The surface of these samples is very smooth and homogeneous, that is, no topographic contrast caused by variations of the SE yield resulting from local tilt of the specimen surface or from local variations of the secondary emission coefficient is expected.

A short glance on the experimental technique for measuring the spatial distributions of SE1 + SE2

In order to investigate the spatial distributions of SE1 and SE2 quantitatively we combined a scanning electron microscope with an electron emission microscope (e.g., Hasselbach 1971, 1973) (Fig. 1).

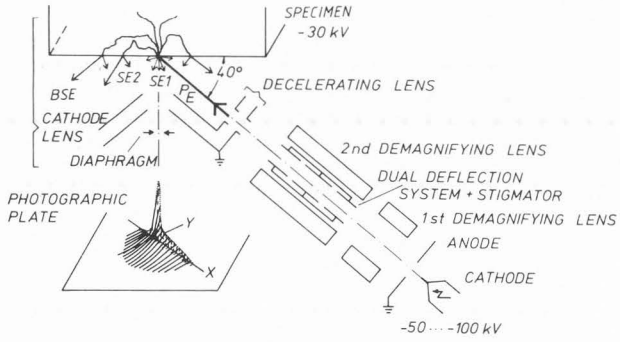

Fig. 1. Experimental set-up

The scanning microscopical column - given on the right hand side of Fig. 1 - produces a spot of 0.3-0.5 µm in diameter on the specimen surface at energies of the primary beam of 20 - 70 keV (smaller spot diameters could not be achieved due to the the large working distance of 12 cm of the second demagnifying lens). The secondaries released by the impinging primaries and by the backscattered electrons are accelerated by the high electric field in front of the specimen surface which is generated by the potential applied to the specimen with respect to the anode and the wehnelt electrode of the cathode lens. This lens projects a magnified, spatially resolved image of the distribution of SE1+SE2 on the fluorescent screen or photographic plate. The diaphragm in its back focal plane with its diameter of 100 µm improves the resolution limit of the cathode lens to a value of 0.1 µm. This is due to the fact that with decreasing diameter, the diaphragm cuts off the high energetic tail of the energy distribution of the secondaries (e.g., a diaphragm of 100 µm in diameter cuts off most of the secondary electrons with energies larger than about 2.5 eV (Dietrich and Seiler 1960; Möllenstedt and Lenz 1963; Schwarzer 1975;)). This leads to a lower chromatic aberration. Additionally the aperture prevents all SE3 and BSEs from reaching the photographic plate. Due to the oblique angle of incidence of the primaries the spatial distribution of the secondaries is not rotationally symmetric around the point of incidence. According to the Monte Carlo calculations of Reimer (1968), Shimizu and Murata (1971) and Murata (1973, 1974) one is expecting a spatial distribution similar to that given schematically in the plane of the fluorescent screen/photographic plate of Fig. 1. In the following this distribution will be called "point response function". The x-z plane is the symmetry plane of this distribution. When this point response function is deflected parallel to the x-direction we observe a line, the "line response function". The intensity distribution

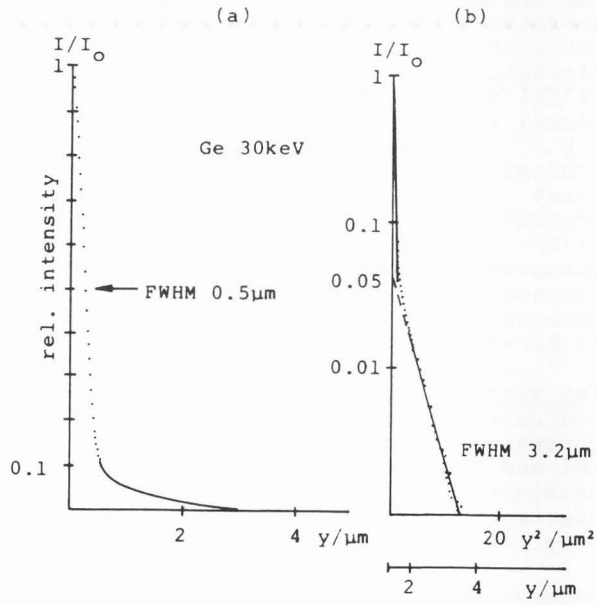

Fig. 2: Densitometric evaluation of a line response function plotted linearly (2a) and in the form of ln (I/I_0) versus y^2 (2b). Note the two abscissa scales y^2 and y in Fig. 2b.

perpendicular to this line response function is symmetrical. We recorded such line response functions photographically for samples of different materials and for different energies of the incident primaries. In order to work in the linear part of the exposure curve of the photographic emulsion the low and high intensity parts of the line response function were recorded in two micrographs differing in their exposure times by a factor of 16. As an example, a densitometric evaluation of such a line response function is given in Fig. 2.

Such photographically recorded line response functions represent the integral of the corresponding point response function in scanning direction. This becomes intelligible by the following consideration: Imagine an intersection perpendicular to a line. When the line is written on the photographic plate, all parts of the SE distribution pass the intersection successively and contribute to the exposure.

Some remarks on contrast and its definition

In scanning microscopy three principal contrast forming mechanisms exist: topographic contrast, material contrast and crystal orientation contrast. We report quantitative data of the proportion of the secondary electron currents

$$C^* = SE1/(SE1 + SE2)$$

which is identical with the fraction of the total secondary signal that carries useful contrast at the resolution limit (e.g., Joy 1984). It characterizes the signal to background ratio in each pixel ("single pixel contrast") and is closely related to contrast in its conventional definition.

The conventional definition of contrast C - originating from light microscopy - is given by the following formula:

$$C = (I_1 - I_2)/(I_1 + I_2) \qquad [1]$$

where I_1 is the intensity in two adjacent pixels 1 and 2. As already mentioned, while in transmission microscopy either with light or electrons the intensities I_1 and I_2 originate from the interior of the corresponding pixels, in scanning electron microscopy only a fraction of the image forming secondaries - the SE1 - are released inside of each pixel area. The intensities I_1 and I_2 - which are equivalent to the total current of secondaries released when the electron beam is incident on a certain pixel - are composed of the three parts SE1, SE2 and SE3. The BSE induced SE2 and SE3 contain no highly resolved information of the pixel just scanned.

The fraction of the video signal corresponding to the SE2 and SE3 secondaries is only slowly varying from pixel to pixel. Therefore, if we substitute in [1] for the intensities the corresponding secondary electron currents when the pixels 1 and 2 are hit by the electron probe, it is remarkable that in the numerator the amplitudes of the video signal corresponding to SE2 and SE3 cancel to a first approximation while in the denominator they add up. This leads to a drastic reduction of the contrast available in scanning microscopy on bulk specimens.

In the following we want to calculate the influence of the SE2 only on contrast using our experimental data. We do not take into account the component SE3 at all and justify this by the fact that the component SE3 may be reduced or prevented from reaching the detector in principle (Peters 1982a,b; Reimer and Volbert 1979) and that in most modern scanning microscopes precautions are taken to reduce the SE3 substantially. Neglecting the SE3 totally means that our results give an upper limit for the contrast available.

Imagine a flat homogeneous surface where just one pixel differs in its secondary emission coefficient - caused, e.g., by local contamination - from the adjacent pixels. The contrast definition [1] may be described then very illustratively by the following symbolical equation:

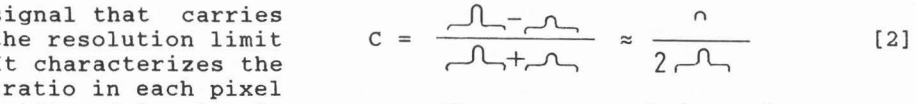

[2]

The narrow peak in each case represents the SE1 while the broad distribution symbolizes the SE2. The right hand side of the equation is valid when we approximate the SE1 contributions of the two pixels in the denominator by:

$$SE1_1 + SE1_2 \approx 2\,SE1_1 \approx 2\,SE1_2 \qquad [3]$$

This is justified by the fact that we only neglect the comparatively small quantity $SE1_1 - SE1_2$ compared to the whole denominator. The portions SE2 are exactly the same due to the fact that we use flat homogeneous specimens.

Our "single pixel contrast" C^* is related to the conventional contrast definition by:

$$C^* = SE1/(SE1 + SE2) = \frac{\cap}{\sqcap} \qquad [4]$$

$$C \approx (SE1_1 - SE1_2)/2(SE1 + SE2)$$

$$= 1/2\,(C_1^* - C_2^*) \qquad [5]$$

The enormous decrease of contrast C

due to the SE2 is the reason for the various attempts to prevent not only the SE3 but also the SE2 electrons from reaching the detector (Hasselbach et al. 1983) or to subtract a signal proportional to the SE2 current delivered by an extra BSE detector - multiplied by a suitably chosen constant factor - from the total signal produced by the SE-detector (Crewe and Lin 1976, Volbert 1982a, 1982b). Another method to enhance contrast is to enrich the SE1 fraction in the video signal by a suitable preparation of the specimens (Peters 1982a, Peters et al.1983).

Quantitative evaluation of the experimental line response functions

The line response functions were evaluated using a Zeiss Axiomat light optical densitometer microscope connected on-line with a microcomputer. An example of such a function has already been shown in Fig. 2a. If we plot the relative intensity I/I_0 as a function of the distance y^2 from the center of the distribution logarithmically (Fig. 2b), we see that the high intensity part ($y \to 0$) (corresponding to the SE1) as well as the extended low intensity portion ($y \to \infty$) (corresponding to the SE2) may be approximated by straight lines, i.e., by Gaussian distributions. The normalized intensity I/I_0 may be approximated by:

$$\frac{I}{I_o} = \frac{N_s \cdot \left[exp\left(-\frac{y^2}{a^2} \cdot ln2\right)\right] + N_u \cdot \left[exp\left(-\frac{y^2}{b^2} \cdot ln2\right)\right]}{N_s + N_u} \quad [6]$$

where N_s in the formula is the maximum of the Gaussian distribution characterizing the spatial distribution of the SE1, 2a the full width at half maximum (FWHM) of the SE1, N_u the maximum of the SE2 distribution and 2b the corresponding FWHM of the SE2. The fact that both distributions are of Gaussian type makes it possible to describe our experimental data with two parameters, the FWHM and their relative maximum height N_u/N_s only. These characteristic parameters are easily extracted from such plots. The FWHM of the distribution SE2 for an infinitely fine impinging primary electron beam (i.e., the δ-function response), $SE2_\delta$ is given by:

$$SE2_\delta = \sqrt{(SE2)^2 - (SE1)^2} \quad [7]$$

The knowledge of $SE2_\delta$ is necessary for the calculation of the influence of the BSE-induced decrease of contrast at the resolution limit of the SEM and renders it possible to calculate exact values for the exposure correction in electron beam lithography (proximity effect correction) (Hasselbach and Rieke 1978).

Table 1 summarizes the characteristic parameters of our experimental Gaussian line response functions: the FWHM of the impinging probe, the FWHM of the SE2 δ-function response ($SE2_\delta$) and the relative peak heights N_u/N_s of the SE2 and SE1 distributions for energies of the primaries in the range of 20 - 70 keV for Si, Ge and Ag. The FWHM of the impinging primary probe was 0.3 ± 0.03 µm for Si and 0.5 ± 0.03 µm for Ge and Ag. N_u/N_s of course depends on this size.

Table I

	Si		Ge		Ag	
probe diam. FWHM	0.3±0.03µm		0.5±0.03µm		0.5±0.03µm	
kV	$SE2_\delta$ [µm]	N_u/N_s	$SE2_\delta$ [µm]	N_u/N_s	$SE2_\delta$ [µm]	N_u/N_s
20	2.9	0.035	1.52	0.120	.92	0.158
30	6.0	0.022	3.21	0.052	1.50	0.132
40	9.3	0.017	4.60	0.042	2.44	0.084
50	12.6	0.013	6.48	0.031	3.34	0.061
60	17.5	0.009	8.28	0.025	4.24	0.050
70	21.5	0.007	10.10	0.020	5.12	0.040

Table 1. Characteristic parameters (FWHM of incident probe = FWHM of SE1 in our approximation, FWHM of BSE induced secondaries for an infinitely fine impinging primary beam $SE2_\delta$, relative height of the SE2 distribution N_u/N_s) of the Gaussian line response functions for materials of different atomic number Z and energy of the primaries. Angle of incidence 50° to the surface normal.

In order to determine the total number of electrons belonging to the fractions SE1 and SE2 we only have to calculate the integral of the Gaussian line response functions using the characteristic parameters as given in table 1. We obtain for the integrated intensities of:

$$SE1 = N_S \int_{-\infty}^{\infty} exp\left(-\frac{y^2}{a^2} ln\,2\right) dy = \alpha\, N_S\, a \quad [8]$$

$$SE2 = N_U \int_{-\infty}^{\infty} exp\left(-\frac{y^2}{b^2} ln\,2\right) dy = \alpha\, N_U\, b \quad [9]$$

for a and b > 0; α= const.;

and the single pixel contrast:

$$C^* = SE1/(SE1+SE2) = N_s\, a/(N_s\, a + N_u\, b)$$

$$= 1/(1+\Sigma) \quad [10]$$

$$\text{with } \Sigma = N_u\, b/N_s\, a \quad [11]$$

The values of Σ calculated from our experimental data are subject to an error of about 20%. They are given in table 2:

Table II

E [keV]	Si	Ge	Ag
20	0.34	0.37	0.29
30	0.44	0.33	0.40
40	0.52	0.39	0.41
50	0.55	0.40	0.41
60	0.52	0.41	0.42
70	0.50	0.40	0.41

Table 2. Experimental values of Σ for Si, Ge and Ag for energies of the impinging primaries ranging from 20-70 keV. Angle of incidence 50° to the surface normal.

The influence of BSE induced secondaries on contrast in the SEM

The values of Σ do not depend - within the limits of the accuracy of our measurements - on the energy of the primary electrons. Using the mean values of Σ we obtain for the single pixel contrast:

$$C^*_{Si} = 0.68$$

$$C^*_{Ge} = 0.72$$

$$C^*_{Ag} = 0.72$$

i.e., the maximum of the single pixel contrast neither depends on the energy of the primaries nor on the material within the overall uncertainty of our measurements.

When a smooth homogeneous specimen is imaged in the SEM, the single pixel contrast is constant, i.e., according to [5] no structures at all are visible in SEM micrographs. We assume now that inside the area of an isolated pixel the secondary emission is higher by 20 % for example (the cause may be an enhanced secondary emission due to a slight tilt of the surface or a locally increased SE emission coefficient) and calculate the contrast C:

$$C = 1/2\ (C_1^* - C_2^*)$$

$$\approx 1/2(1.2 \cdot SE1/(SE1+SE2) - SE1/(SE1+SE2))$$

using that $C^* = SE1/(SE1+SE2) = 0.7$

$$C = 1/2(\ 0.2 \cdot SE1/(SE1+SE2)) = 0.07$$

An increase of the emission of 20% in an isolated pixel results in a very faint contrast of only 7 % in the corresponding SEM micrograph.

These considerations are valid on the assumption that none or only a negligible part of the BSE's leave the specimen surface inside the pixel just scanned, i.e., at the resolution limit of the microscope. When the microscope works at low magnification, the pixel size increases and now more and more of the BSEs leave the surface inside the pixel. The secondaries induced by these BSEs now carry information about this pixel and become part of the SE1 signal. The lower the magnification, the more the contrast available increases (e.g., Joy 1984). This increase of contrast as a function of the pixel size may be easily deduced from our experimental data as well. In order to do this one has to integrate the SE2 contributions emerging in- and outside of the pixel area separately. The portion emerging inside is added to the SE1 contribution when the contrast is calculated.

The increase of contrast with decreasing magnification is faster for specimens of high atomic number due to the lower maximum range of the electrons within these materials. For the same reason topographic contrast increases when the microscope is operated with lower beam voltages (Pease 1967; Pawley 1986). Therefore, low voltage SEM will possibly provide the ultimate in high resolution topographic images of biological samples (Pawley 1984a, b) in the future.

The β values

The total secondary yield SE_T consists of that induced by the primaries and the one induced by the reemerging BSEs:

$$SE_T = SE1 + SE2 = SE1 + \beta\eta \cdot SE1$$

$$= SE1 \cdot (1+\beta\eta) \qquad [12]$$

where η is the backscattering coefficient. The mean BSE-induced secondary yield is higher by a factor β (Everhart 1958; Kanter 1961a,b; Seiler 1967, 1983; Drescher et al. 1970) compared to the emission induced by a primary electron since the energy distribution of the BSEs is broad and their average energy lower than that of the primaries. Last but not least their lower average emergence angle to the surface leads to the enhanced secondary yield. Thus, β is given by the following relation:

$$\beta = (1/\eta)(SE2/SE1) = \Sigma/\eta \qquad [13]$$

The values for Σ (see Table 2) are identical with βη. These values of Σ do not differ significantly from each other for the different energies of the prima-

ry electrons. Therefore we calculate the β value using the mean value of Σ for each element. The values of η for an angle of incidence of 50° to the surface normal known from literature are (Kanter 1957, Drescher et al. 1970, Niedrig 1982): $\eta_{Si} = 0.31$; $\eta_{Ge} = 0.44$; $\eta_{Ag} = 0.54$ yielding β values of:

$$\beta_{Si} = 1.55; \quad \beta_{Ge} = 0.88; \quad \beta_{Ag} = 0.74;$$

However, in order to compare these values with results at normal incidence of the electron beam, we have to take into account that according e.g., to Bronshtein and Denisov (1967) and Bronshtein and Dolinin (1968), β decreases for increasing angle of incidence. For Be and Pb at 50° these authors measured about 60 % of its peak value at normal incidence. We assume that this behaviour is approximately valid for Si, Ge and Ag as well since we are unaware of quantitative experimental data concerning these elements. Then our experimental β values for normal incidence are:

$$\beta_{Si} = 2.58; \quad \beta_{Ge} = 1.46; \quad \beta_{Ag} = 1.23$$

Compared with experimental values of Kanter (1961b), Bronsthein and Denisov (1967), Bronshtein and Dolinin (1968) and Seiler (1967) who report β values of about 5, our experimental values are substantially smaller. Our mean secondary electron yield β of one backscattered electron is of the order of $1<\beta<3$ which corroborates the low β values of the order of 2 experimentally found by Drescher et al. (1970) and Reimer and Drescher (1977).

Summary and Prospect

We calculate from our emission microscope measurements of the BSE induced line response functions the yield of SE1 and SE2 from bulk flat specimens. Using these values, we determine the "single pixel contrast C*= SE1/(SE1+SE2)". The results represent upper limits of contrast at the resolution limit since our experimental SE2 yields are lower limits because they were gained on flat samples. The surface of real SEM specimens is rough, i.e., more BSEs leave the surface of such a specimen, e.g., near edges and release SE2. The BSE's may even penetrate the specimen again thus contributing a second time to the SE2 yield (Hasselbach and Rieke 1976).

As an example we derive the contrast according to its conventional definition for the case of an isolated pixel with 20% higher secondary emission rate. The resulting contrast of 7 % only demonstrates the problem of low contrast in SEM micrographs caused by the scattering properties of the specimen.

The β values of $1<\beta<3$ deduced from our measurements corroborate the results of Drescher et al. (1970) and Reimer and Drescher (1977). They are substantially smaller than the values of about 5 which are found in the older literature reviewed, e.g., by Seiler (1967).

The outstanding advantage of the emission microscope method is that the SE2 and SE1 current emerging from the specimen surface is visualized directly and can be measured spatially resolved for every single pixel - not only for flat specimens but for specimens with rough convoluted topography as well -. The method is even more powerful: not only increased SE2 yield due to topography e.g., edge brightening (Hasselbach and Rieke 1976, Wells 1977,1986) is visible and measurable of course, but also that due to different materials, crystallographic orientations and even local charging of specimen structures (Hasselbach 1988). Therefore the emission microscope method will allow us to make a large step forward to the quantitative understanding of contrast formation in SEM micrographs.

References

Bronshtein IM, Denisov SS. (1967). Secondary electron emission of aluminium and nickel obliquely incident primary electrons. Sov. Phys.-Solid State 9, 731.

Bronshtein IM, Dolinin VA. (1968). The secondary electron emission (SEE) of solids at large angles of incidence of the primary beam. Sov. Phys.-Solid State 9, 2133-2140

Crewe AV, Lin PSD. (1976). The use of backscattered electrons for imaging purposes in a scanning electron microscope. Ultramicroscopy 1, 231-238.

Dietrich W, Seiler H. (1960). Energieverteilung von Elektronen, die durch Ionen und Elektronen in Durchstrahlung an dünnen Folien ausgelöst werden. Z. Physik 157, 576-585.

Drescher H, Reimer L, Seidel H. (1970). Rückstreukoeffizient und Sekundärelektronen-Ausbeute von 10-100 keV-Elektronen und Beziehungen zur Raster Elektronenmikroskopie. Z. f. Angew. Physik 29, 331-336.

Everhart TE. (1958). Contrast formation in the SEM. Ph. D. dissertation Cambridge University.

Everhart TE, Wells OC, Oatley CW. (1959). Factors affecting contrast and resolution in the scanning electron microscope. J. Electr. Control 7, 97-111.

George EP, Robinson VNE. (1976). Dependence of SEM contrast upon electron

penetration. Scanning Electron Microsc. 1976;I: 17-26.

Hasselbach F. (1971). Untersuchung der Verbreiterung von fokussierten Elektronenstrahlen durch Streuung in dünnen und dicken Objekten mit dem Elektronenemissionsmikroskop. 15. Tagung für Elektronenmikroskopie 1971 in Karlsruhe. Abstract published in Mikroskopie 28,(1972), 352.

Hasselbach F. (1973). Messung der Ortsverteilung von gestreuten Elektronen in Durchstrahlung und Reflexion im Elektronenemissionsmikroskop. Dissertation Universität Tübingen.

Hasselbach F, Rieke U. (1976). Emission microscopical investigation of the edge brightening effect in scanning electron microscopy. 6th European Congress on Electron Microscopy, Jerusalem, 1976. TAL International Publishing Company, Jerusalem: Vol. I, 296-298.

Hasselbach F, Rieke U. (1978). Emission microscopical investigation of the proximity effect in electron beam lithography. 9th International Congress on Electron Microscopy, Toronto 1978. JM. Sturgess, VI.Kalnins, FP. Ottensmeyer, GT. Simon (eds.), published by the Microscopical Society of Canada, University of Toronto, Toronto, Ontario M5S 1A1: Vol.I, 166-167.

Hasselbach F, Rieke U. (1982). Spatial distribution of secondaries released by backscattered electrons in silicon and gold for 20-70 keV primary energy. Proc. 10th International Congress on Electron Microscopy, Hamburg, 1982. Published by the Deutsche Gesellschaft für Elektronenmikroskopie e. V., Frankfurt, 1982. Vol. I, 253-254.

Hasselbach F, Rieke U, Straub M. (1983). An imaging secondary electron detector for the SEM. Scanning Electron Microsc. 1983;II: 467-478.

Hasselbach F, Krauß H-R. (1985). Spatial distribution of secondaries released by backscattered electrons in germanium and silver for 20-70 keV primary energy. Optik Suppl. 1, 28.

Hasselbach F. (1988). The emission microscope, a valuable tool for investigating the fundamentals of the scanning electron microscope. Scanning Microsc. 2, 41-56.

Joy DC. (1984). Beam interactions, contrast and resolution in the SEM. Journal of Microscopy 136, Pt 2, 241-258.

Kanter H. (1957). Zur Rückstreuung von Elektronen im Energiebereich von 10-100 keV. Ann. Phys. 20, 144-166.

Kanter H. (1961a). Energy dissipation and secondary emission in solids. Phys. Rev. 121, 677-681.

Kanter H. (1961b). Contribution of backscattered electrons to secondary electron formation. Phys. Rev. 15, 681-684.

Möllenstedt G, Lenz F. (1963). Electron Emission Microscopy. Advan. Electron. 18, 251-329.

Murata K. (1973). Monte Carlo calculations on electron scattering and secondary electron production in the SEM. Scanning Electron Microsc. 1973: 267-276

Murata K. (1974). Spatial distribution of backscattered electrons in the scanning electron microscope. J. Appl. Phys. 45, 4110-4117.

Niedrig H.(1982). Electron backscattering from thin films. J. Appl. Phys. 53, R15-R49.

Pawley JB. (1984a). Low voltage SEM. J. Microscopy 13, 387-410.

Pawley JB. (1984b). SEM at low beam voltage. EMSA (San Francisco Press, San Francisco) 42, 440-443.

Pawley JB. (1986). Low voltage scanning electron microscopy. Electron Optical Systems, JJ. Hren, FA. Lenz, E. Munroe, PB. Sewell, SA. Bhatt (eds.), published by SEM Inc., AMF O'Hare (Chicago) pp. 253-272.

Pease RFW. (1965). The determination of the area of emission of reflected electrons in a scanning electron microscope. J. Sci. Instr. 42, 158-159.

Pease RFW. (1967). Low-voltage scanning electron microscopy. Record of IEEE 9th Symposium on Electron Ion and Laser Beam Technology, Berkeley 1967, RFW. Pease (ed.), San Francisco Press, 176-187.

Peters K-R. (1982a). Conditions required for high quality high magnification images in secondary electron-I scanning electron microscopy. Scanning Electron Microsc. 1982; IV: 1359-1372.

Peters K-R. (1982b). Validation of George and Robinson SE1 signal theorem. Implication for ultrahigh resolution SEM on bulk untilted specimens. 40th Ann. Proc. Electron Microscopy Soc. Amer., Washington DC, 1982. GW Bailey (ed.), Claitors Publ. Div., Baton Rouge, LA. 368-369.

Peters K-R, Schneider BG, Papermaster DS. (1983). Ultrahigh resolution scanning electron microscopy of a periciliary ridge complex of frog retinal rod cells. J. Cell. Biol. 91, 273a.

Reimer L, Seidel H, Gilde H. (1968). Einfluß der Elektronendiffusion auf die Bildentstehung im Raster-Elektronen-Mikroskop. Beitr. elektronenmikroskop. Direktabb. Oberfl. G. Pfefferkorn (ed.), 2, 52.

Reimer L. (1968). Monte-Carlo-Rechnungen zur Elektronendiffusion. Optik 27, 86-98.

Reimer L, Drescher H. (1977). Secondary electron emission of 10-100 keV electrons from transparent films of Al and Au. J. Phys. D: Appl. Phys. 10, 805-815.

Reimer L, Volbert B. (1979). Detector system for backscattered electrons

by conversion to secondary electrons. Scanning 2, 238-248.

Robinson VNE. (1974). The origins of the secondary electron signal in scanning electron microscopy. J. Phys. D: Appl. Phys. 7, 2169-2173.

Schwarzer R. (1975). Der Einfluß von Loch- und Ringblenden auf die Energieverteilung der Elektronen im Emissionselektronenmikroskop. Optik 44, 61-78.

Seiler H. (1967). Einige aktuelle Probleme der Sekundärelektronenemission. Z. Angew. Phys. 22, 249-263.

Seiler H. (1968). Die physikalischen Aspekte der Sekundärelektronenemission für die Raster-Elektronen-Mikroskopie. Beiträge Elektr. Direktabb. Oberflächen, G. Pfefferkorn (ed.), 1, 27-52.

Seiler H. (1983). Secondary electron emission in the scanning electron microscope. J. Appl. Phys. 54, R1-R18.

Shimizu R, Murata K. (1971). Monte Carlo calculations of the electron-sample interactions in the scanning electron microscope. J. Appl. Phys. 42, 387-394.

Volbert B. (1982a). Signal mixing techniques in Scanning electron microscopy. Scanning Electron Microsc. 1982; III:897-905.

Volbert B. (1982b). True surface topography: the need for signal mixing. In: Proc. 10th International Congress on Electron Microscopy, Hamburg, 1982. Published by Deutsche Gesellschaft für Elektronenmikroskopie e.V, Frankfurt 1982. Vol. 1, 233-234.

Wells OC. (1977). Penetration effect at sharp edges in the scanning electron microscope. Scanning 1, 58-60.

Wells OC. (1986). Reduction of edge penetration effect in the scanning electron microscope. Scanning 8, 120-126.

Yamamoto T. (1976). Measurement of the emission area of backscattered electrons. Phys. Stat. Sol. (a)38, 361-368.

Discussion with Reviewers

Klaus-Ruediger Peters: What is the difference between SE1, defined by you as being produced by "impinging electrons" of the probe, and SE-I, defined by others as being produced by "unscattered" electrons of the probe during their first scattering event?

Authors: We define as SE1 all secondaries that are released inside the area of the impinging primary beam, including the secondaries that are produced by multiple scattered electrons reemerging by chance inside the primary probe diameter. All these electrons carry useful information about the pixel just scanned. This is well known and causes the increase of contrast in SEM micrographs when the magnification is lowered. We admit that this definition of SE1 is not adequate for a scanning microscope working in the very high resolution mode where the diameter of the impinging electron probe is comparable or even substantially smaller than the range of the secondary electrons of a few nanometers only.

Klaus-Ruediger Peters: Did you observe in your experiments at lower voltages a dramatic increase of SE1 production as suggested by Monte Carlo computations from Joy (1985)?

Authors: No, the resolution of our cathode lens is only about 100 nm, far less than a fraction of 1 nm which would be necessary to observe the SE1 production spatially resolved. Secondly, our measurements were performed not at really low beam voltages but at 20-70 kV.

Klaus-Ruediger Peters: What caused your SE1 to emerge in Ag at a 100 nm larger distance from the probe site than in Si? It was shown (Seiler, 1967; Joy, 1985) that the SE scattering (diffusion) range varies only a little (1-2x) over a wide range of accelerating voltage or atomic number of the specimen. Do you suggest that the scattering (diffusion) range proper of your SE1 increases 100x in a specimen of higher atomic number composition?

Authors: There is a misunderstanding: The FWHM of our probe diameter is, within the limits of error, identical with the FWHM of the SE1 (take into consideration our definition of SE1 and our large probe diameter). In the text the FWHM of the SE1 distribution and FWHM of the impinging probe means the same.

Klaus-Ruediger Peters: How do your data on the scattering range of SE1 relate to range measurements made by others using high magnification topographic contrasts as an analytical tool (Broers 1974; Peters 1982a, 1984a,b, 1985). These authors measured and interpreted the range of SE produced by the "incoming" electrons of the probe to be 100x shorter than you suggest.

Authors: We fully agree with the range measurements of the authors cited in your question. Our paper contains no range measurements of secondaries. The contradiction given in your question is due to the misunderstanding which we tried to clarify in the answer to the last question.

Klaus-Ruediger Peters: The probe diameter is expected to vary with the accelerating voltage. Could you please provide some data on actual probe diameters used for the range measurements in Table 1? Did you measure probe

diameters with a method independent from the range of BSE or SE?
Authors: The actual probe diameters (FWHM) were 0.3±0.03 µm for Si and 0.5 ±0.03 µm for Ge and Ag for all acceleration voltages used. We measured the probe diameters independently from the range of the BSE's by using the thin film method which is described in the answer to the first question of Murata.

Klaus-Ruediger Peters: What accelerating voltages were used in Table 1 for FWHM data of SE1?
Authors: The FWHM of the SE1 (= FWHM of the impinging probe) was - within the limits of error - constant for each element irrespective of the accelerating voltage (20-70 kV) used.

Kenji Murata: In Fig. 2 there seems to be a large contribution of the secondary electrons generated by backscattered electrons in the central region where you obtained the width of the SE1 distribution, especially for heavy elements (see, for example Fig.3 in Murata (1974)). Could you estimate the error induced by this contribution?
Authors: Yes, we have a contribution of secondary electrons generated by backscattered electrons to the SE1 (SE1 as defined in the answer to the question of K.-R. Peters). Let us estimate this error for the worst case, an Ag specimen at 20 keV. The peak intensity of the SE2 for Ag at 20 keV is about 16% of that of the secondaries that are generated by the entering primary electron beam. Our 50% height of the distribution is therefore exact only within about 8%. These 8% of systematic error lead to an error in the FWHM of the SE1 for the Ag specimen of less than 60 nm. This in turn leads to an error of the FWHM of our SE2 response functions for an infinitely fine impinging beam of less than ±2,5%. In order to prove experimentally that the influence of the BSE-induced secondaries in the central region does not influence our results significantly we compared the FWHM of SE1 which we obtained from a bulk gold specimen and a thin film specimen at 20 keV (20nm of Au on a 20 nm of formvar). The FWHM which we obtained in both cases was the same within our limits of error. The error decreases with increasing energy of the primary beam and decreasing atomic number of the specimen.

Kenji Murata: Could you check if your experimental data of SE2 follow the law of $SE2 \propto E^n$ which is similar to the equation of the electron range? Please find the value of n for Si, Ge and Ag. This will be useful also in electron beam lithography.
Authors: For the different elements the relation between the FWHM in µg/cm² and E in keV is given by:
Si: FWHM= $5.8\ E^{1.59}$
Ge: FWHM= $11.7\ E^{1.45}$
Ag: FWHM= $16.3\ E^{1.37}$

Kenji Murata: Could you comment on the reason why the values of Σ do not depend very much on the primary beam energy?
Authors: Σ is equivalent to η times β. η is almost independent of the primary beam energy in the energy range in question. Since our experimental values of Σ are subject to an error of about 20%, we can only conclude that - within these limits of error - our β values do not depend on the primary beam energy.

Kenji Murata: According to Kanter, the β value is enhanced at least by a factor of 2 owing to longer travelling path lengths of the backscattered electrons (BSE's) in the secondary emission region near the surface, which results from the cosine law distribution of BSE's. Another enhancement factor is the lower energies of the BSE's which have a higher emission capability of secondary electrons. Your β values for Ge, and Ag are smaller than 2. Please comment on this discrepancy.
Authors: We do not know why our β values for Ge and Ag are smaller than 2. Let us mention here that there are contradictory values of β in literature. Reimer and Drescher (1977) also report experimental values of β for Al and Au smaller than 2. They state that their calculated values of 2.92 for Al and 2.52 for Au represent upper limits.

V.N.E. Robinsons comment: 1. The experimental set up they have used is entirely unsatisfactory for what they are attempting to measure. The column they have used produces a 0.3 to 0.5 micron diameter beam on the surface of the specimen. The reaction that they are trying to separate, is one which occurs either side approximately 3 nano meters, that is the interaction volume produced in their experiment is about one hundred times larger than the effect, they are trying of observe. Even though they reduce this value to about 0.1 microns they are totally unable to separate SE1 and SE2 in that experimental situation. As such, any conclusion they make become meaningless.

In order to perform such an experiment properly they would have to produce a demagnified image of their cathode, which has a diameter of approximately 3 nano meters. This needs then to be magnified in its entirety onto the plate. This they have not done. It then becomes pointless to speculate about the worth or otherwise of the rest of their mathematics.

Authors: We are not at all trying to separate the reaction which occurs within 3 nm around the impinging primary beam, as you write in your comment. We measure the spatial distribution of the secondaries that are released by the **backscattered electrons reemerging from the surface of a bulk specimen**. The emission microscope gives us the possibility to visualize directly these distributions spatially resolved. You may find micrographs that show from which parts of the specimen these secondaries are emitted - also for the special cases, e.g., of edge brightening - in the paper of Hasselbach and Rieke 1976, Hasselbach 1988. The dimensions of the area on the surface of the specimen where these secondaries are released may be characterized - this is a rule of thumb - by the range of the scattered electrons in the specimen. For silicon and 25 keV electrons this range is of the order of 6 μm and at 70 keV of more than 70 μm (see e.g., Reimer 1984) and not in the 3 nm range. For quantitatve measurements in these μm-dimensions our probe diameter of 0.3-0.5 μm and the resolving power of our cathode lens of 0.1 μm is sufficient. The dimensions of the reaction volume of 3 nm, as given in your comment, is roughly identical with the range of the secondary electrons in a metallic specimen and not with the range of the **fast scattered** electrons.

Additional References

Broers AN. (1974). Recent advances in scanning electron microscopy with lanthanum hexaboride cathodes. Scanning Electron Microsc. 1974; I: 9-18.

Hasselbach F, Rieke U. (1976). Emission microscopical investigation of the edge brightening effect in scanning electron microscopy. 6th. European Congress on Electron Microscopy, Jerusalem, 1976. TAL International Publishing Company: Vol. I, 296-298.

Joy DC. (1985). Resolution in low voltage scanning electron microscopy. J. Microsc. 140, 283-292.

Peters K-R. (1984a). Scanning electron microscopy: Contrast at high magnification. In: Microbeam Analysis - 1984, Roming AD and Goldstein JI. (eds.) San Francisco Press Inc, San Francisco pp 77-80.

Peters K-R. (1984b). Generation, collection and properties of an SE-I enriched signal suitable for high resolution SEM on bulk specimens. In: Kayser DF, Niedrig H, Newbury DE, Shimizu R. (eds.), Electron Beam Interactions with Solids for Microscopy, Microanalysis and Microlithography. Scanning Electron Microscopy Inc., AMF O'Hare, pp 363-372.

Peters K-R. (1985). Working at higher magnification in scanning electron microscopy with secondary and backscattered electrons on metal coated biological specimens and imaging cell membrane structures. Scanning Electron Microsc. IV, pp 1519-1544.

Reimer L. (1984). Scanning electron microscopy. Springer Series in Optical Sciences, JM Enoch, DL. MacAdam, AL. Schawlow, K. Shimoda, T. Tamir (eds.). Springer-Verlag Berlin Heidelberg New York Tokio. p. 100.